

# Topological Approach for Analyzing and Modeling the Aerodynamic Hysteresis of an Airfoil

Tao Cui<sup>1</sup>, Wenhao Liao<sup>1</sup> and Daren Yu<sup>1</sup>

**Abstract:** Aerodynamic hysteresis is of practical importance for the flying airfoils. Motivated by the problem of global description on the hysteresis behaviors, this paper proposes a topological approach to analyze and model the hysteresis behaviors exhibited in the airfoil flow from a viewpoint of dynamic system theory. The approach is based on the topological invariant rules of singular points under topological mapping. It is able to theoretically explain such discontinuous hysteresis phenomena, and make consistent and accurate predictions of the hysteresis behaviors in the airfoil flow. The model results have shown that the present model is in good agreement with the available experimental data.

**Keywords:** Topological invariant, modeling, aerodynamic hysteresis, airfoil.

## 1 Introduction

### 1.1 Background

In the field of fluid dynamics, an area of significant practical importance is the study of airfoils. An airfoil refers to the cross sectional shape of an object designed to generate lift when moving through a fluid. Fundamentally, an airfoil generates lift by diverting the motion of fluid owing over its surface in a downward direction, resulting in an upward reaction force by Newton's third law. Airfoil aerodynamics is very important for both military and civilian applications. The applications include propellers, sailplanes, man-carrying/man-powered aircraft, high-altitude vehicles, wind turbines, unmanned aerial vehicles, and micro air vehicles.

### 1.2 Motivation and objective

In recent years there has been an increasing demand to extend the range of airfoils' flight conditions to high angle-of-attack regimes and high-amplitude maneuvers. As the angle of attack of an airfoil to the incoming flow increases beyond a certain

---

<sup>1</sup> Harbin Institute of Technology, Harbin, Heilongjiang, People's Republic of China

point, flow stall will occur, then the massive flow separation on the airfoil surface will be observed and there will be a sharp drop in the lift and increase in the drag. In certain cases the flow will be accompanied by an aerodynamic hysteresis between flow stall and recovery. Aerodynamic hysteresis is of practical importance for the flying airfoils because it produces sharp changes in the lift and drag, and produces widely different values of lift and drag for a given angle of attack; this will have great impact on the flight performance and safety. The physical mechanism of hysteresis phenomena has been investigated in many studies. However, the hysteresis phenomena have been analyzed in an isolated manner, and there exists a need for unified approaches to analyze systematically the global hysteresis behavior at different flight angle of attack and Reynolds number.

A suitable methodology for global analysis would, in addition to providing quantitative, global information, also contribute towards safer piloting procedures, airfoil model structure determination and control system design (Shaopu and Yongjun 2009). The method should also be able to predict and explain such discontinuous hysteresis phenomena. In the theory of dynamic system, bifurcation analysis and catastrophe theory approach have been developed to accomplish the above objectives.

In this paper, a topological approach is proposed to analyze and model the hysteresis phenomena exhibited in the airfoil flow from a viewpoint of dynamic system theory. It can make consistent and accurate predictions of the hysteresis behaviors in airfoils, and is in good agreement with available experimental data.

### **1.3 Previous works**

Hysteresis phenomena have been found to be relatively common for airfoils at low Reynolds numbers. Whereas the aerodynamic hysteresis associated with the pitching motion of airfoils, also known as dynamic stall, has been investigated extensively (Hu, Zifeng and Igarashi 2007; Biber 2005), hysteresis phenomena observed for static stall of an airfoil have received much less attention. In one of the early works, Mueller (1985) investigated the aerodynamic characteristics of Lissaman 7769 and Miley M06-13-128 airfoils at low Reynolds numbers, and found that both airfoils produced hysteresis loops in the profiles of measured coefficients of lift and drag forces when they operated below chord Reynolds numbers of 300,000. Hoffmann (1991) reported his results for an experimental study for flow past a NACA 0015 airfoil at  $Re$  250,000. Hysteresis loop in the data for the aerodynamic coefficients was observed. Hysteresis has also been reported by Biber and Zumwalt (1993) for a two-element GA(W)-2 airfoil. Mittal and Saxena (2002) conducted a numerical study to predict the aerodynamic hysteresis near the static stall angle of a NACA 0012 airfoil in comparison with the experimental data of Thibert, Grand-

jacques and Ohman (1979). More recently, Zifeng and Hirofumi (2008) conducted a experiment study to investigate the aerodynamic characteristics of a NASA low speed GA(W)-1 airfoil at the chord Reynolds number of  $Re=160,000$  and aerodynamic hysteresis was observed for the angles of attack close to the static stall angle of the airfoil.

#### 1.4 Paper outline

To achieve the above objectives, we will first introduce the available experimental results of the Lissaman 7769 airfoil in section 2, and identify the central idea of the topological analysis and modeling approach in Sections 3 and 4.

## 2 Experimental results

Mueller (1985) investigated the aerodynamic characteristics of the Lissaman 7769 airfoil (Fig. 1), and found the airfoil produced hysteresis loops in the profiles of measured coefficients of lift and drag forces when it operated at the chord Reynolds numbers of 150,000, 200,000 and 290,000 respectively as shown in Fig. 2 (a,b,c).



Figure 1: Lissaman 7769 airfoil geometry

Fig. 2(a) shows the section lift and profile drag coefficients vs angle of attack for  $Re=150,000$  for the Lissaman 7769 airfoil. Hysteresis is present at this Reynolds number as the air foil angle of attack varies. For angles from about 0 to 10 deg, the coefficients of lift and drag forces are only one value for a given angle of attack. Between about 10 and 20 deg, catastrophe and hysteresis results in a sharp drop in the lift and increase in the drag. When the chord Reynolds number was increased to 200,000, the hysteresis region was reduced as shown in Fig. 2(b). On this condition, the abrupt decrease in lift occurred at about 20 deg for increasing angle of attack and the lift jumped up when the angle of attack was decreased to about 17 deg. At a chord Reynolds number of about 290,000 as shown in Fig. 2(c), the abrupt decrease in lift occurred at about 21 deg and jumped back up at about 20 deg.

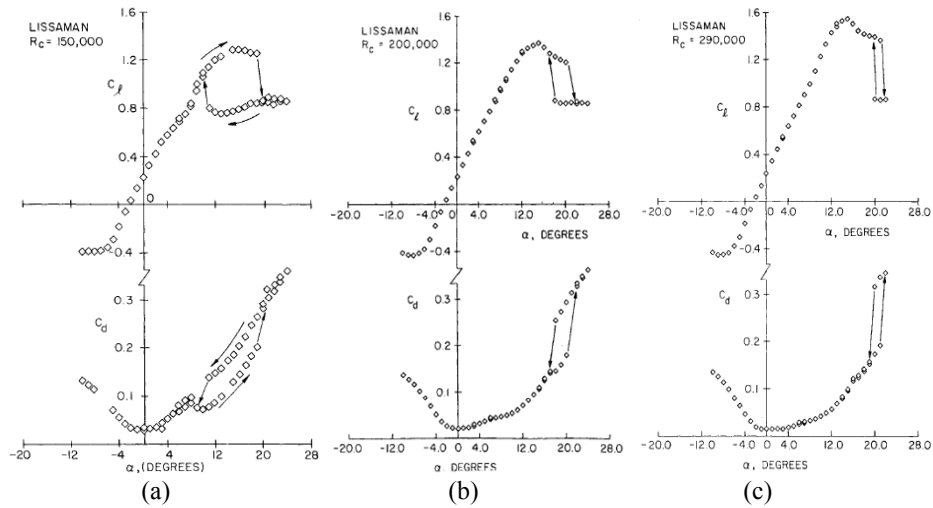


Figure 2: Lift and drag coefficients vs angle of attack for different Reynolds numbers

### 3 Topological analysis

A central idea of the work in this section is to analyze the catastrophe and hysteresis characteristic exhibited in the airfoil flow by applying topological approaches in the framework of dynamic system theory.

#### 3.1 Singular points and the topological invariant rules

The transitions between flow stall and recovery in the airfoil flow has shown catastrophe and hysteresis characteristics in the lift and drag. Physically, at low angles of attack, the flow is completely attached on both the lower and upper surfaces of the airfoil. When the angle of attack increases to a critical value, the flow on the upper surface begins to separate near the trailing edge of the airfoil, and then a flow stall occurs accompanying by a catastrophe jump in the lift and drag. For the decreasing angles of attack, the flow will remember its past history and the separation reattaches at another critical angle of attack. The ability of the flow to remember its past history is responsible for its hysteresis behavior.

The occurrence of catastrophe and hysteresis in the process of flow stall and recovery means there is a qualitative change in the flow structure of the airfoil. According to the theory of dynamic system, the critical conditions where flow stall or recovery begins to occur are mathematically correspondent to the singular points, which are special points at which all the partial derivatives simultaneously vanish; it is this

set of singular points that contains the significant behavior of the physical process. In mathematics, Whitney's singularity theory is a tool to study the singular points. It is one of the accessible entry points to both highly abstract areas of mathematics and to applied fields such as dynamical systems and bifurcations. Whitney in his book "Mappings of the Plane into the Plane" proposed that there were general rules in the distribution of singular points in the variable space, that is, the topological character of singular points is invariant under topological mapping.

With the topological invariant rules, Whitney observed two types of singularities are stable and persist after small deformations of the mapping. Thus Whitney has provided some normal forms of different kinds of singularities; these norm forms of singularities may help to explore the distribution laws of singular points. Whitney has given significant information on singularities of generic mappings; this information can be used to study large numbers of diverse phenomena and processes in all areas of science. According to Whitney's singularity theory, a mapping of a surface onto a plane associates to each point of the surface a point of the plane. If a point on the surface is given coordinates  $(X, U)$  on the surface, and a point on the plane is given coordinates  $(Z, W)$ , then the mapping is given by a pair of functions  $Z=F(X, U)$  and  $W=G(X, U)$ . The mapping is said to be smooth if these functions are smooth (i.e., are differentiable for a sufficient number of times, such as polynomials). Thus Whitney observed two types of singularities (fold and cusp) are stable and persist after small deformations of the mapping.

### ***3.2 Classification of singularities with topology***

Whitney's theory gives significant information on singularities of generic mappings; this simple idea is the whole essence of Thom's classification theorem. Thom's classification theorem is a special topic within the broader domain of dynamic system theory that pertains to sudden discontinuous changes of events. It was mainly developed by Thom (1972). In the following years, Zeeman (1977) and Poston and Stewart (1978) introduced and advocated broad interdisciplinary applications of Thom's classification theorem. It provides a detailed mathematical description of how the surface geometry of the functional changes with control parameters. Around a critical point, the local geometry of the energy functional is described by a certain catastrophe function whose normal form is determined by the number of zero eigenvalues in the Hessian matrix and the control parameters. Thom's classification theorem can deal with complex systems with properties of discontinuities directly without reference to any specific underlying mechanism. This attractive property makes it especially appropriate for the modeling of systems whose inner workings may not be known, as is usually the case in the study of complex systems.

The theorem applied ideas from differential topology and topological dynamics to classification of singularities and introduced methods that described how to determine any type of singularity within a list of singularities. In Thom's classification theorem, two notions are very important. One is codimension and the other is unfolding. Codimension is a topological conception, and it is invariant under topological transformation. Two functions which are equivalent have the same codimension (Trotman and Zeeman 1976). With this invariance, singularities may be classified. After determining the codimension, the next step is to obtain normal mathematic descriptions by constructing topological transformation, which involves another important notion as unfolding. A function is topological invariant to its unfolding, therefore, The character of all isolated singularities can be investigated by examining truncated unfoldings (Guckenheimer 1973). The unfolding emerges as a complete generalization of the function and the codimension as the number of different functions that can be added to the singularity list.

In Thom's classification theorem, the equilibrium points of a potential function with non-zero eigenvalues of the Hessian are called Morse critical points. The Morse Lemma states that at these points the qualitative properties of the function are determined by the quadratic part of the Taylor expansion of this function. This part can be reduced to the Morse canonical form by topology transformation. If at an equilibrium point the Hessian degenerates, so that at least one of the eigenvalues is zero, the type of equilibrium point cannot be determined. The equilibrium points of a potential function with zero eigenvalues (singular points) are also called non-Morse critical points. The core of the catastrophe theory lies in finding a canonical form for an arbitrary potential function  $V$  in a neighborhood of a non-Morse critical point. This is accomplished by conceiving suitable variable changes that render it locally possible to standardize the form of  $V$  without altering any of its qualitative properties and in particular its critical point structure. Appropriate transformations are diffeomorphisms. Since a higher order Taylor expansion is essentially needed to describe the qualitative properties, although the dimension of the variables is arbitrary, the Thom Lemma states that one can split up the function in a Morse and a non-Morse part, and the latter consists of variables representing the  $k$  eigenvalues of the Hessian that become zero, and  $k$  is the codimension. The Morse part contains the  $n - k$  remaining variables. Consequently, the Hessian contains a  $(n - k) \times (n - k)$  sub-matrix representing a Morse function. Therefore, it suffices to study the part of  $k$  variables. The canonical form of the function at the non-Morse critical point thus contains two parts: a Morse canonical form of  $n - k$  variables, in terms of the quadratic part of the Taylor series, and a non-Morse part. The latter can be put into canonical form called the catastrophe germ by topology transformation, which is obviously a polynomial of degree 3 or higher. Since the Morse part does not change

qualitatively under small perturbations, it is not necessary to further investigate this part. The non-Morse part, however, does change. Generally, the non-Morse critical point will split into a non-Morse critical point, described by a polynomial of lower degree, and Morse critical points, or even exclusively into Morse critical points; this event is called a morsification. So the non-Morse part contains the catastrophe germ and a perturbation that controls the morsifications. Then the general form of a Taylor expansion  $V(X,U)$  at a non-Morse critical point of a  $n$ -dimensional function can be written as:

$$V(X,U) = CG(x_1, x_2, \dots, x_k) + PT(x_1, x_2, \dots, x_k; u_1, u_2 \dots u_l) + \sum_{i=k+1}^n \varepsilon_i x_i^2 \quad (1)$$

where  $CG(x_1, x_2, \dots, x_k)$  denotes the catastrophe germ,  $PT(x_1, x_2, \dots, x_k; u_1, u_2 \dots u_l)$  denotes the perturbation germ with a  $m$ -dimensional space of parameters,  $l$  is the dimension of independent variables (corank), and in the Morse part  $\varepsilon_i = \pm 1$ . In catastrophe theory the germs with  $l \leq 4$  are mathematically presented. These germs are the starting point of the infinite set of so-called simple real singularities, whose catastrophe germs are given by the series  $A_k^{\equiv} x^{k+1}, k \geq 1$  and  $D_k^{\pm} \equiv x^2 y \pm k^{k-1}, k \geq 4$ . Thus the elementary catastrophes, known as fold, cusp, swallowtail, butterfly, hyperbolic umbilic, elliptic umbilic and parabolic umbilic, are normalized to classify different singularities. Thom's Theorem was rigorously demonstrated by Mather (1966) and Arnold (1968). Later a more complete categorization was carried out by Varian (1979), Arnold (1992) and Gusein-Zade (1995). In fact, these elementary classifications have provided certain mathematical models of the diverse singular systems. Many valuable applications have since appeared in different research areas such as physics (Carricato and Duffy 2002; Brito, Fiolhais and Paixao 2003), chemistry (Slawomir and Zdzislaw 2006; Wales 2001), biology (Torres 2001) and social sciences (Holyst, Kacperski and Schweitzer 2000; Yiu and Cheung 2006).

### **3.3 Analysis of the experimental results**

In this section the topological conceptions in Thom's Theorem will be illustrated to interpret the catastrophe and hysteresis phenomena. From the experimental data as shown in Fig. 2, there are two independent variables of Reynolds numbers and angle of attack that govern the catastrophe and hysteresis process, and there exist two kinds of flow modes in the flowfield of the airfoil, then the codimension is two. Correspondingly the catastrophe and hysteresis phenomena may be topologically interpreted and explained applying the cusp model.

Cusp model describes a three-dimensional response surface consisting of one state and two independent variables. The dynamics of the system is recorded in the

vertical movements of the state variable as a result of the changes in its two control dimensions, whose potential function in three-dimensional space is

$$V(Z, \beta, \alpha) = Z^4 + \beta Z^2 + \alpha Z \quad (2)$$

The equilibrium surface  $M$  is described as

$$4Z^3 + 2\beta Z + \alpha = 0 \quad (3)$$

Then project  $M$  into the control space by eliminating  $x$  to obtain the bifurcation set

$$8\beta^3 + 27\alpha^2 = 0 \quad (4)$$

A classical graphical illustration of the cusp model is provided in Fig. 3, which shows how discontinuous changes in the dependent behavioral responses can occur with smooth changes in the asymmetry factor  $\alpha$  and the splitting factor  $\beta$ . The equilibria of the cusp form a three-dimensional surface. For certain values of  $\alpha$  and  $\beta$  (between the bifurcation lines) two stable equilibria occur (and one repelling maximum). Increasing the variable on the  $\alpha$ -axis results in a sudden jump in the variable on the  $Z$ -axis. Decreasing the variable on the  $\alpha$ -axis results in a jump downward. The phenomenon that the jump upward occurs at a higher value of the variable on the  $\alpha$ -axis than the jump downward is called hysteresis. When the variable on the  $\beta$ -axis is increased, the jump between low and high values on the  $Z$ -axis becomes more extreme, and this is called divergence.

Under the direction of the topological geometry space for the cusp catastrophe, we redraw the experimental data in Fig. 2 as shown in Fig. 4. Obviously, the experimental data may present the basic topological characteristic of the cusp catastrophe. Firstly, the catastrophe and hysteresis phenomena may be obviously explained according to the topological geometry space for the cusp catastrophe, that is, when the airfoil operates at Reynolds numbers of 150,000, 200,000 and 290,000, there will be catastrophe and hysteresis in the lift  $C_l$  and drag  $C_d$ , and the corresponding bifurcation lines may form a typical fork bifurcation as shown in Fig. 3. Secondly, the experimental results may also reveal the bifurcation phenomenon, that is, when the airfoil operates at higher Reynolds number, no hysteresis is present and the airfoil performs smoothly (Corresponding experimental data are not provided). The bifurcation phenomenon exhibited in the airfoil flow may also be explained by the topological geometry space for the cusp catastrophe. As shown in Fig. 3, when  $\alpha=0$  and  $\beta$  is changed, the airfoil will perform a supercritical pitchfork bifurcation, where the independent variables  $\alpha$  and  $\beta$  are respectively the topological transformation function of the Reynolds number and angle of attack. It can be seen

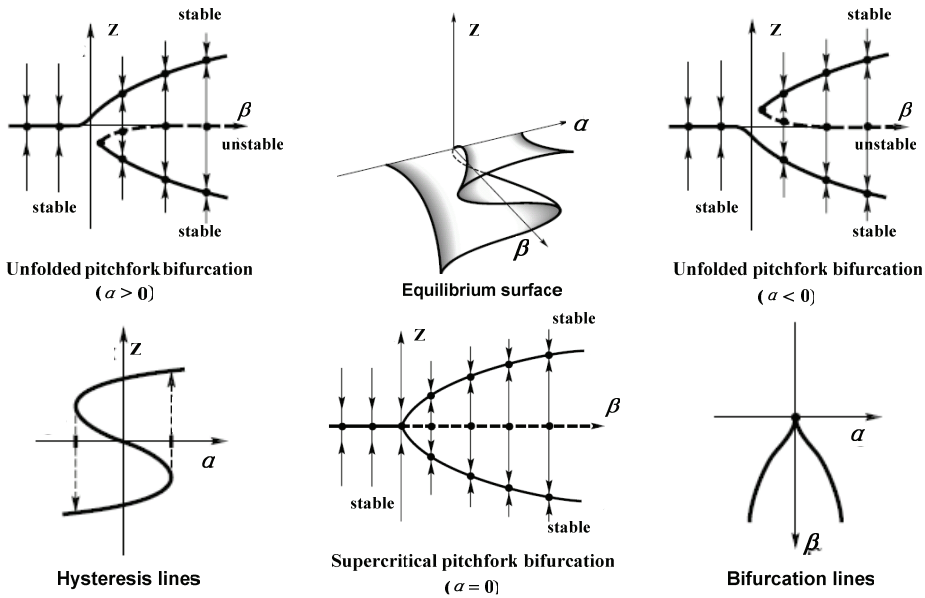


Figure 3: Topological geometry space for the cusp catastrophe

that in this bifurcation both the upper and lower branch of the pitchfork bifurcation have stable equilibrium points, which corresponds to the two stable states: static flow stall and recovery. But the middle branch is shown dashed to denote that it is unstable, which corresponds to the unstable state of the instantaneous flow separation and reattach. Because the state is unstable, they are regarded as “inaccessible”. Another branch in described as  $\beta > 0$  has only stable equilibrium points, which corresponds to the state of flow recovery at high Reynolds numbers, and no catastrophe and hysteresis occur on this condition. It is interesting to find that when  $\alpha \neq 0$ , the pitchfork bifurcation unfolds, that is, there will be a hysteresis along Reynolds number which will cause a sudden change from one stable branch to the other stable branch, e.g., from the lower to the upper branch when Reynolds number is decreased to the critical point.

Analysis of the above show that the discontinuous hysteresis phenomena exhibited in the airfoil flow may be well explained by applying topological approaches in the framework of dynamic system theory.

#### 4 Topological modeling

As known, well-developed statistical techniques, such as regression analysis and multivariate analysis, have been developed to model smooth, continuous change

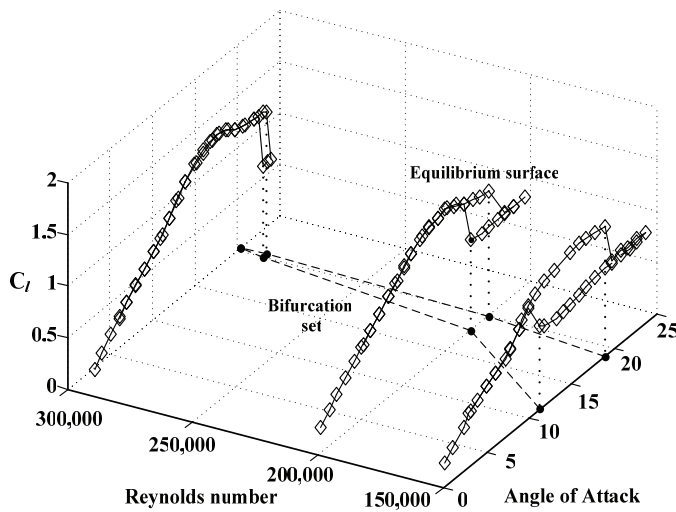


Figure 4: Equilibrium surface and bifurcation set of the Lissaman 7769 airfoil

with empirical data. For systems exhibiting complex nonlinear behaviors such as catastrophe, bifurcation and chaos, corresponding analysis and model approaches should be introduced (Ananthakrishna 2005; Chen, Gan, and Chen 2008; Ferretti, Casadio and Di 2008; Loeven and Bijl 2008; Nishioka, Furutuka, Tchouikov and Fujimoto 2002; Parussini and Pediroda 2007; Parussini and Pediroda 2008; Pichler and Mang 2000; Sousa 2005; Volokh 2001; Yuan and Zhang 2008). In this section, we attempt to mathematically model the discontinuous catastrophe and hysteresis phenomena exhibited in the airfoil flow with the available experimental data.

#### 4.1 Central idea

In Thom's Theorem, the model approaches are mainly developed for deterministic systems. An ever persistent problem is the absence of statistical procedures for detecting the presence of a catastrophe in any given body of numerical or experimental data. Thus catastrophe models have become associated in many minds with reckless speculation and intellectual irresponsibility. Cobb (1980) tried to solve this problem by developing stochastic catastrophe theory. Cobb showed that, by using stochastic differential equations, there is a cusp family of probability density functions. In his theory, the deterministic behavior of the dynamic system can be made stochastic and put in the form of a stochastic differential equation  $V_{sto}(Z, U)$ , and a polynomial function is constructed to be the topological transformation function. A specially defined probability density function  $p(x|u) = \xi \exp[-V_{sto}(x, u)]$

is presented by solving the corresponding Fokker–Planck equation yielding to estimate the parameters of the polynomial topological transformation function. A stable equilibrium corresponds to a mode and an unstable equilibrium corresponds to an antimode of the probability density function. That is, a stable equilibrium state is a point of high probability. A change in the number of equilibrium states corresponds to a change in the number of modes and antimodes of the probability density function. Given the probability density functions of the cusp model, the control variables can be estimated with empirical data by using maximum likelihood estimation. Cobb’s basic idea of introducing statistic process into catastrophe theory has been well developed and applied in many directions. Several other modeling procedures have been proposed. Hartelman (1998) outlined a more flexible version of Cobb’s original program using a more reliable optimization routine, allows to constrain parameter values and to employ different sets of starting values. Further, Hartelman (1997) developed a method based on kernel densities. This method allows nonlinear transformations of the variables of the cusp model. Other methods for fitting the catastrophe models, such as polynomial regression technique (Guastello 1992) and GEMCAT I and II (Oliva, DeSarbo and Day 1987, Lange, Oliva and McDade 2000) have also be proposed.

**4.2 Model procedures and results**

In fact, the statistical fit of catastrophe models to empirical data is often difficult and is a developing area of research. For some cases when the bifurcation set of a cusp catastrophe system is approximately symmetrical, the above statistic procedure may be of validity to fit data to the model. However, in most cases, the symmetrical conditions can not be satisfied. Then a direct fit of this bifurcation set to the data is not satisfactory (Vaessen 1995). Unfortunately, in this case the symmetrical conditions may not be satisfied as shown in Fig. 4.

We may apply topological method to solve this problem, that is, to fulfill the needs for a symmetrical bifurcation set, we may firstly construct certain topological transformation to transform the origin shape of the bifurcation set to a symmetrical geometry. In this way, the symmetrical conditions as discussed above may then be satisfied. With this consideration, we make the first topological transformation by radial basis function neural network to shape the bifurcation set of the stall and recovery of the airfoil into a symmetric configuration as shown in Fig. 5. The transformation may be described as

$$\begin{cases} w_1 = Re \\ w_2 = NN_1(Re, \delta) \end{cases} \tag{5}$$

where  $NN_1$  is the transformation function by radial basis function neural network,

Re is the Reynolds number, and  $\delta$  is the angle of attack. According to the theory of RBF neural networks, the transform from the input layer space to the hidden layer space is nonlinear, while the transform from the hidden layer space to the output space is linear. That is to say, the mapping between the input and output is nonlinear, and that the output of the network is linear for the adjustable parameters. Then the weights of the network can be found directly by the linear equations, so the learning speed can be quickened greatly. Also it can avoid the problem of converging to local minimum. The training algorithms for an RBF neural network have been divided into two stages. First, using unsupervised learning algorithm, the centers for hidden layer nodes can be determined. Second, after the centers are fixed, the widths are determined in a way that reflects the distribution of the centers and input patterns. Once the centers and widths are fixed, the weights between the hidden and output layers can be trained.

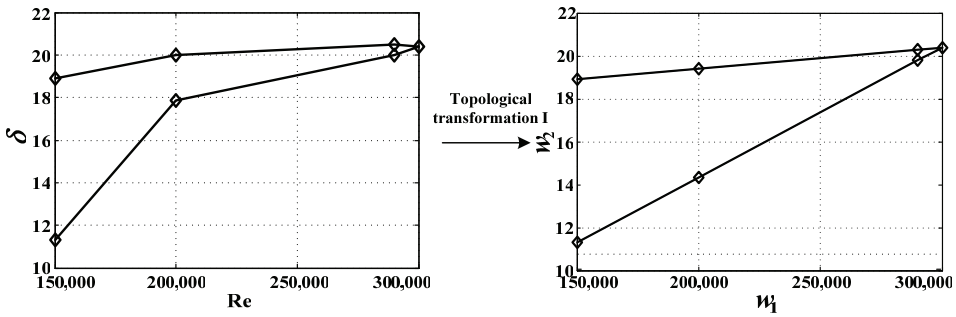


Figure 5: Topological transformation of the bifurcation set to a symmetrical geometry

The second step is another kind of topological transformation as smooth coordinate transformation. The coordinate system  $Q(w_1, w_2)$  changes into  $R(v_1, v_2)$ , and this express as follows

$$\begin{cases} v_1 = l_1 w_1 + l_2 w_2 - \phi \\ v_2 = m_1 w_1 + m_2 w_2 - \varphi \end{cases} \quad (6)$$

where  $\phi$  and  $\varphi$  are the  $Q$  point value in the coordinate system  $R(v_1, v_2)$ , and  $l_1, l_2, m_1, m_2$  are the direction cosine from the coordinate system  $Q(w_1, w_2)$  to the coordinate  $R(v_1, v_2)$ , this process is shown in Fig. 6.

The third step is an analytical topological transformation in which the target function is described as Eq. (4) according to catastrophe theory. Let  $\bar{k}$  be the absolute

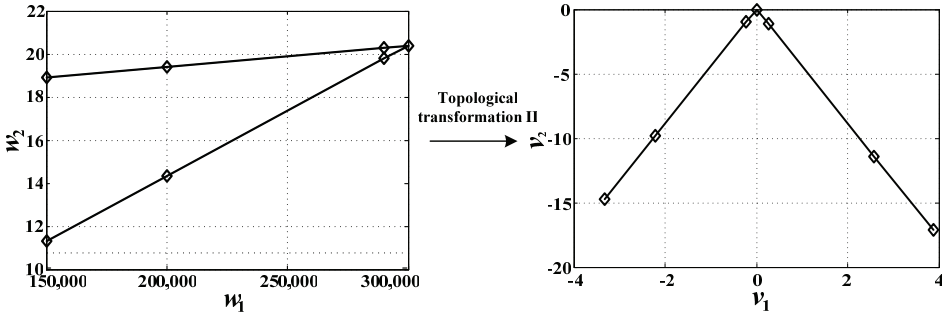


Figure 6: Coordinate transformation

value of the two symmetric curves' approximate slope, and by constructing the following topological transformation function

$$\begin{cases} \alpha = \sqrt{\frac{2}{27}k}v_1 \\ \beta = -\sqrt[3]{\frac{1}{8}v_2^2} \end{cases} \quad (7)$$

In this process, we obtain the model results of the bifurcation set of the airfoil. The bifurcation set are exactly the stability boundaries of the airfoil's stall and recovery. The model results of the bifurcation set are shown in Fig. 7, and we can see that the model results of the bifurcation set can fit the experimental data very well.

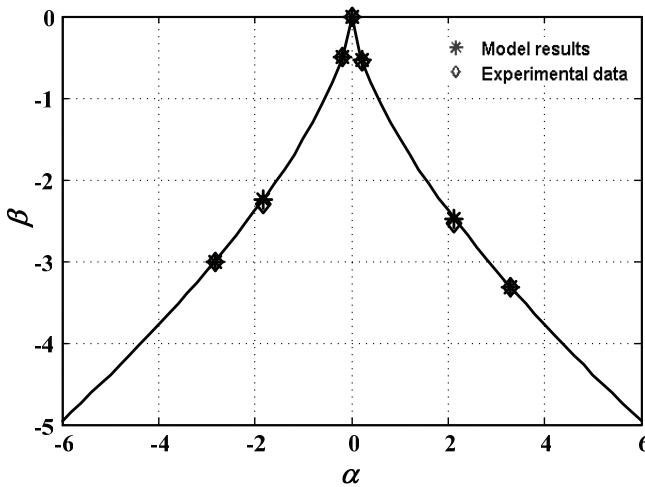


Figure 7: Model results of the bifurcation set of the airfoil

The above steps have made an accurate fitting of the bifurcation set  $\{(Re, \delta)\}$  of the airfoil to the bifurcation set  $\{(\alpha, \beta)\}$  of the cusp model. Finally, we will use parts of the experiment data to fit the equilibrium surface  $\{(Re, \delta, C_l)\}$  of the airfoil (Fig. 4) to the equilibrium surface  $\{(\alpha, \beta, Z)\}$  of the cusp model. The final model step is to find a topological transformation function

$$Z = Z(Re, \delta, C_l) \quad (8)$$

together with the topological transformation functions (Obtained by the above steps)

$$\begin{cases} \alpha = \alpha(Re, \delta) \\ \beta = \beta(Re, \delta) \end{cases} \quad (9)$$

to optimize the following integral least-square index  $\Phi$  as (Lange et al. 2000, Oliva et al. 1987)

$$\Phi = \|e_n^2\| = \sum_{n=1}^N [4Z_n^3 + 2\beta_n Z + \alpha_n]^2 \rightarrow 0 \quad (10)$$

where  $N$  is the number of training samples. In this paper, a part of the experimental data shown in Fig. 2 is chosen to train the radial basis function neural network  $NN_2$ , and the radial basis function neural network and the similar training method in the first step are applied to obtain the topological transformation function

$$Z = NN_2(Re, \delta, C_l) \quad (11)$$

Through these steps, the model results of the equilibrium surface are obtained and shown in Fig. 8 with the percentage errors shown in Fig. 9. The percentage error is the model error divided by the corresponding model result and then multiplied by 100%. It appears from the model results that the topological model can fit the available data very well with the maximum percentage errors 3.63% at the training samples.

### 4.3 Model test

An effective topological model of the airfoil should be capable of providing accurate calculation results on the bifurcation set (critical conditions) of the flow stall and recovery. Therefore it is necessary to test the validity of the model on the bifurcation set. With this consideration, we select the origin points in the control surface of the physical system of the airfoil as the test points, which are denoted by  $a_1, a_2, \dots, a_{13}$ ,  $b_1, b_2, \dots, b_{10}$ , and  $c_1, c_2, \dots, c_7$  as shown in Fig. 10. Correspondingly, the model results in the control surface are shown in Fig. 11 where the corresponding points are denoted by  $A_1, A_2, \dots, A_{13}$ ,  $B_1, B_2, \dots, B_{10}$ , and  $C_1, C_2, \dots, C_7$ .

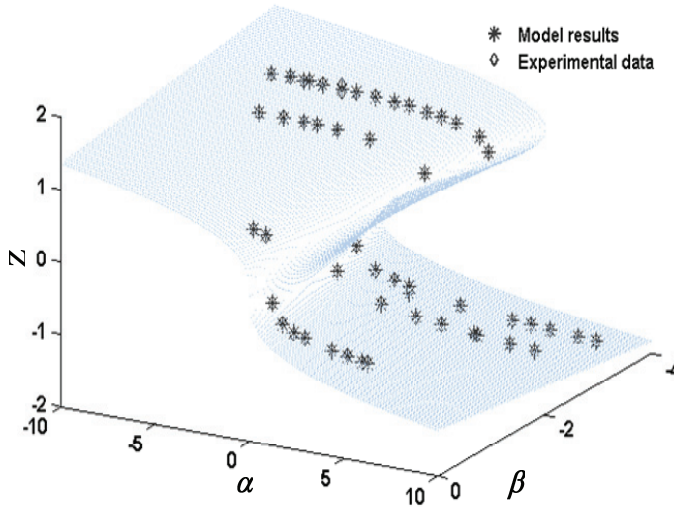


Figure 8: Model results of the equilibrium surface of the airfoil at the training samples

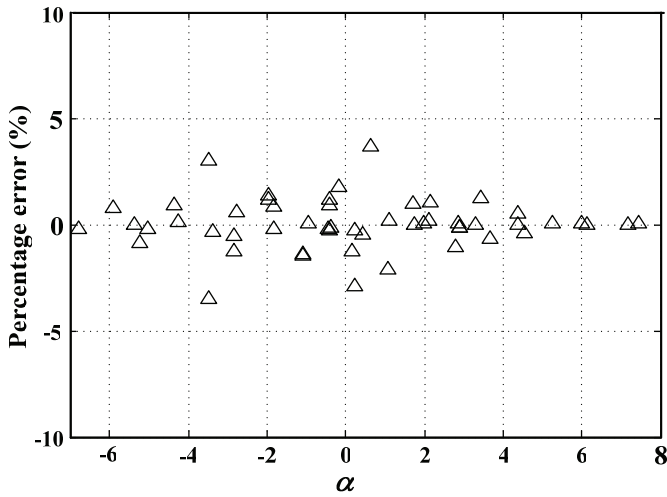


Figure 9: Percentage errors of the model results at the training samples

Comparing the two figures, we may see that the bifurcation points in Fig. 10, such as  $a_3, a_{10}, b_3, b_5, c_3, c_4$ , fit well with the points of  $A_3, A_{10}, B_3, B_5, C_3, C_4$  in Fig. 11, which are also the bifurcation points. Geometrically, the continuous points in Fig. 10 fit well in general direction with the points in Fig. 11 which are also the continuous points. The corresponding points in the two figures are located in the same regions divided by the curves of the bifurcation set. As described above, these results show that the model may provide good prediction on the bifurcation set (critical conditions) of the flow stall and recovery of the airfoil.

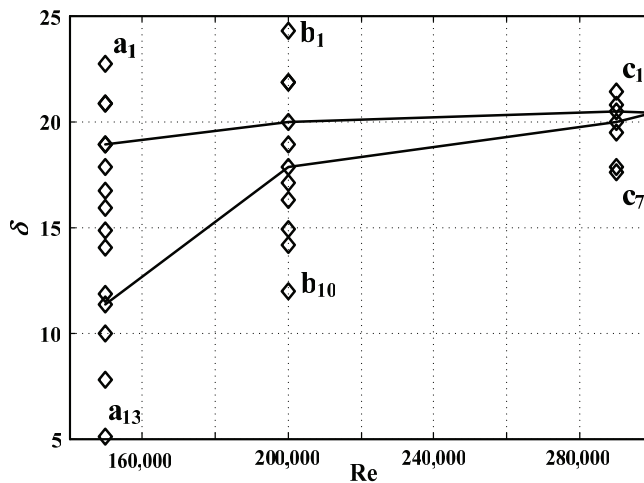


Figure 10: Origin points in the control surface of the physical system of the airfoil

An effective topological model of the airfoil should also be capable of providing accurate calculation results on the equilibrium surface. As shown in Figs. 8-9, the topological model may fit the available data very well at the training samples. However, the performance of the model should be further investigated at the testing samples. In this section, 20% of the experimental data are employed as the testing samples for verifying the predictive accuracy of the model. The test results shown in Figs. 12-13 show that the topological model can fit the available data very well with the maximum percentage errors 8.9% at the testing samples.

### 5 Conclusion

The applicability of topological invariant rules of singular points to the hysteresis behaviors exhibited in the airfoil flow has been investigated. Applying the topological classification conceptions in Thom’s Theorem, the hysteresis, catastrophe

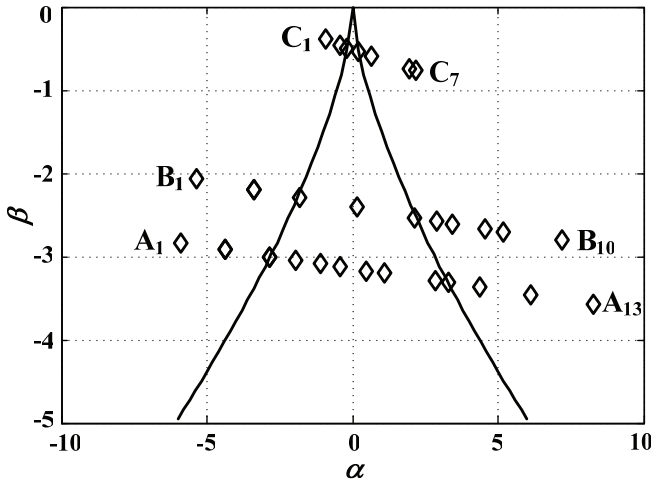


Figure 11: Model results of the points in the control surface of the topological space

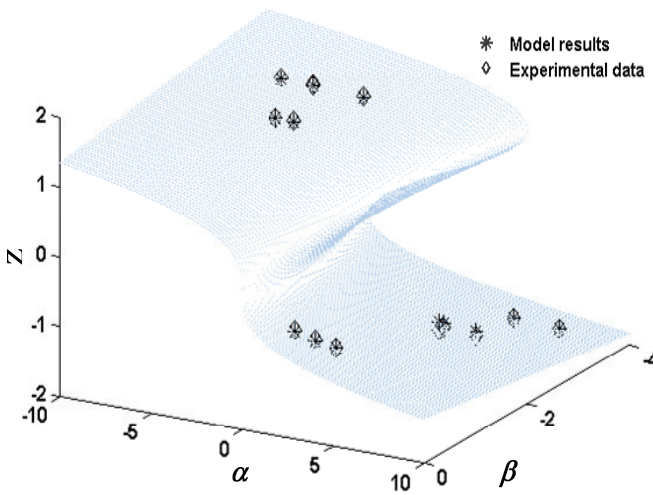


Figure 12: Model results of the equilibrium surface of the airfoil at the testing samples

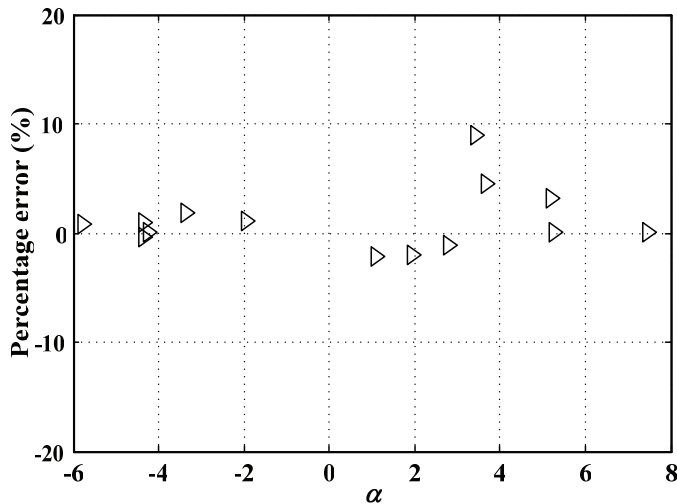


Figure 13: Percentage errors of the model results at the testing samples

and bifurcation phenomena in the airfoil have been theoretically analyzed and explained. Furthermore, a topological approach for fitting the experimental data to the elementary catastrophe model has been proposed. The model has high accuracy comparing to the experimental data. It may be concluded from the present work that the topological approach has provided qualitative and quantitative descriptions on the global hysteresis behaviors of the airfoil.

**Acknowledgement:** Financial supports from the Key Program of the National Natural Science Foundation of China (Grant No. 90816028) and National Science Fund for Distinguished Young Scholars are gratefully acknowledged.

## References

- Ananthkrishna, G.** (2005): A dynamical approach to the spatio-temporal features of the Portevin-Le Chatelier effect. *CMES: Computer Modeling in Engineering & Sciences*, vol. 7, no. 3, pp. 233-239.
- Arnol'd, V. I.** (1992): *Catastrophe Theory, 3rd edition*. Berlin: Springer-Verlag.
- Biber, K.** (2005): Stall hysteresis of an airfoil with slotted flap. *Journal of Aircraft*, vol. 42, no. 6, pp. 1462-1470.
- Biber, K.; Zumwalt, G. W.** (1993): Hysteresis Effect on Wind Tunnel Measurements of a Two-Element Airfoil. *AIAA Journal*, vol. 31, no. 2, pp. 326-330.

- Brito, L.; Fiolhais, M.; Paixao, J.** (2003): Cylinder on an incline as a fold catastrophe system. *European Journal of Physics*, vol. 24, no. 1, pp. 15-23.
- Carricato M.; Duffy, J.** (2002): Catastrophe analysis of a planar system with flexural pivots. *Mechanism and Machine Theory*, vol. 37, pp. 693-716.
- Chen, Z.; Gan, Y.; Chen, J.** (2008): A coupled thermo-mechanical model for simulating the material failure evolution due to localized heating. *CMES: Computer Modeling in Engineering & Sciences*, vol. 26, no. 2, pp. 123-137.
- Cobb, L.; Watson, B.** (1980): Statistical catastrophe theory: An overview. *Mathematical Modelling*, vol. 1, pp. 311-317.
- Ferretti, E.; Casadio, E.; Di, L. A.** (2008): Masonry walls under shear test: a CM modeling. *CMES: Computer Modeling in Engineering & Sciences*, vol. 30, no. 3, pp. 163-189.
- Guastello, S. J.** (1992): Clash of the paradigms: A critique of an examination of the polynomial regression technique for evaluating catastrophe theory hypotheses. *Psychological Bulletin*, vol. 111, pp. 375-379.
- Guastello, S. J.** (1995): *Chaos, Catastrophe, and Human Affairs: Applications of Nonlinear Dynamics to Work, Organizations, and Social Evolution*. Mahwah: Lawrence Erlbaum Associates.
- Guckenheimer, J.** (1973): *Bifurcation and Catastrophe, in Dynamical Systems*. Manuel M. Peixoto, ed. New York: Academic Press.
- Hartelman, P. A.** (1997): *Stochastic Catastrophe Theory*. PhD. Dissertation, Faculty of Psychologie, University of Amsterdam.
- Hartelman, P. A.; Maas, V. D.** (1998): Detecting and modeling developmental transitions. *British Journal of Developmental Psychology*, vol. 16, pp. 97-122.
- Hoffmann, J. A.** (1991): Effects of freestream turbulence on the performance characteristics of an airfoil. *AIAA Journal*, vol. 29, no. 9, pp. 1353-1354.
- Holyst, J. A.; Kacperski, K.; Schweitzer, F.** (2000): Phase transitions in social impact models of opinion formation. *Physica A*, vol. 285, pp. 199-210.
- Hu, I.; Zifeng, Y.; Igarashi, H.** (2007): Aerodynamic hysteresis of a low-Reynolds-number airfoil. *Journal of Aircraft*, vol. 44, no. 6, pp. 2083-2086.
- Lange, R.; Oliva, T.; McDade, S.** (2000): An algorithm for estimating multivariate catastrophe models: GEMCAT II. *Studies in Nonlinear Dynamics and Econometrics*, vol. 4, pp. 137-168.
- Loeven, G.; Bijl, H.** (2008): Probabilistic Collocation used in a Two-Step approach for efficient uncertainty quantification in computational fluid dynamics. *CMES: Computer Modeling in Engineering & Sciences*, vol. 36, no. 3, pp. 193-212.

- Malgrange, B.** (1966): *Ideals of Differentiable Functions*. Oxford. Oxford University Press.
- Mather, J. N.** (1968): Stability of CPO Mapping III: Finitely Determined Map-Germs. *Publications Mathématiques IHÉS*, vol. 35, pp. 127-156.
- Mittal, S.; Axena, P.** (2002): Prediction of hysteresis associated with static stall of an airfoil. *AIAA Journal*, vol. 38, no. 5, pp. 933-935.
- Mueller, T. J.** (1985): The influence of laminar separation and transition on low Reynolds number airfoil hysteresis. *Journal of Aircraft*, vol. 22, no. 9, pp. 763-770.
- Nishioka, T.; Furutuka, J.; Tchouikov, S. Fujimoto, T.** (2002): Generation-phase simulation of dynamic crack bifurcation phenomenon using moving finite element method based on Delaunay automatic triangulation. *CMES: Computer Modeling in Engineering & Sciences*, vol. 3, no. 1, pp. 129-145.
- Oliva, T.; DeSarbo, W.; Day, D.** (1987): GEMCAT: A general multivariate methodology for estimating catastrophe models. *Behavioral Science*, vol. 32, pp. 121-137.
- Parussini, L.; Pediroda, V.** (2007): Fictitious domain with least-squares spectral element method to explore geometric uncertainties by non-intrusive polynomial chaos method. *CMES: Computer Modeling in Engineering & Sciences*, vol. 22, no. 1, pp. 41-63.
- Parussini, L.; Pediroda, V.** (2008): Investigation of multi geometric uncertainties by different Polynomial Chaos methodologies using a fictitious domain solver. *CMES: Computer Modeling in Engineering & Sciences*, vol. 23, no. 1, pp. 29-51.
- Pichler, B.; Mang, H.** (2000): New insights in nonlinear static stability analysis by the FEM. *CMES: Computer Modeling in Engineering & Sciences*, vol. 1, no. 3, pp. 43-55.
- Poston, T.; Stewart, I.** (1978): *Catastrophe theory and its application*. London: Pitman.
- Shaopu, Y.; Yongjun, S.** (2009): Recent advances in dynamics and control of hysteretic nonlinear systems. *Chaos, Solitons & Fractals*, vol. 40, pp. 1808-1822.
- Slawomir, B.; Zdzislaw, L.** (2006): Quantum chemical topology description of the hydrogen transfer between the ethynyl radical and ammonia (C<sub>2</sub>H+NH<sub>3</sub>)—The electron localization function study. *Chemical Physics Letters*, vol. 426, pp. 273-279.
- Sousa, J.** (2005): Numerical Simulations of unstable flow through a spherical bulge in a 90-degree asymmetrical bend. *CMES: Computer Modeling in Engineering & Sciences*, vol. 9, no. 2, pp. 211-219.

- Thibert, J. J.; Grandjacques, M.; Ohman, L. H.** (1979): *Experimental database for computer program assessment*. TR AR-138, AGARD.
- Thom, R.** (1972): *Stabilité structurelle et morphogénèse*. New York: Benjamin.
- Torres, J. L.** (2001): Biological power laws and Drawin's principle. *Journal of Theoretical Biology*, vol. 209, no. 2, pp. 23-32.
- Trotman, D. J.; Zeeman, C. E.** (1976): *Classification of Elementary Catastrophes of Codimension 5, in Structural stability, the theory of catastrophes and applications in the sciences*. Peter J. Hilton, ed. Berlin: Springer-Verlag.
- Vaessen, G. E. J.; STEIN, H. N.** (1979): The Applicability of Catastrophe Theory to Emulsion Phase Inversion. *Journal of Colloid and Interface Science*, vol. 176, pp. 378-387.
- Varian, H. R.** (1979): Catastrophe Theory and the Business Cycle. *Economic Inquiry*, vol. 17, pp. 14-28.
- Volokh, K.** (2001): Nonlinear analysis of pin-jointed assemblies with buckling and unilateral members. *CMES: Computer Modeling in Engineering & Sciences*, vol. 2, no. 3, pp. 389-400.
- Wales, D. J.** (2001): A microscopic basis for the global appearance of energy landscapes. *Science*, vol. 293, no. 20, pp. 67-70.
- Yiu, K.; Cheung, S.** (2006): A catastrophe model of construction conflict behavior. *Building and Environment*, vol. 41, no. 4, pp. 438-447.
- Yuan, X.; Zhang, H.** (2008): Nonlinear Dynamical Analysis of Cavitation in Anisotropic Incompressible Hyperelastic Spheres under Periodic Step Loads. *CMES: Computer Modeling in Engineering & Sciences*, vol. 32, no. 3, pp. 175-184.
- Zeeman, E. C.** (1977): *Catastrophe theory*. München, Amsterdam: Addison-wesley.
- Zifeng, Y.; Hirofumi, I.; Mathew, M.** (2008): An experimental investigation on aerodynamic hysteresis of a low-Reynolds-number airfoil. *46th AIAA Aerospace Sciences Meeting and Exhibit*, Reno, Nevada.

